J. Biochem. 122, 556-562 (1997)

Hairpin Structure of an RNA 28-mer, Which Contains a Sequence of the Enzyme Component of a Hammerhead Ribozyme System: Evidence for Tandem G:A Pairs That Are Not of Side-by-Side Type[1]

Taiichi Sakamoto,* Gota Kawai,† Masato Katahira,* Mi Hee Kim,* Yoichiro Tanaka,* Yasuyuki Kurihara,* Toshiyuki Kohno,‡ Satoru Watanabe,§ Shigeyuki Yokoyama,§ Kimitsuna Watanabe,† and Seiichi Uesugi*,[2]

*Department of Bioengineering, Faculty of Engineering, Yokohama National University, Hodogaya-ku, Yokohama 240; †Department of Chemistry and Biotechnology, Graduate School of Engineering, The University of Tokyo, Hongo, Bunkyo-ku, Tokyo 113; ‡Mitsubishi Kasei Institute of Life Sciences, Minamiooya 11, Machida, Tokyo 194; and §Department of Biophysics and Biochemistry, School of Science, University of Tokyo, Hongo, Bunkyo-ku, Tokyo 113

Received for publication, March 17, 1997

An RNA 28-mer (Rz28) was obtained as a major product by *in vitro* transcription with T7 RNA polymerase of a promoter-template DNA, which contains a sequence for the enzyme component, RNA 24-mer (Rz24), of a mutant hammerhead ribozyme system. Sequence analysis and enzymatic probing study showed that Rz28 has 4 extra nucleotides at the 3′-terminus, the sequence of which is complementary to that of the 5′-terminal sequence of Rz24, and forms a stable hairpin structure. NMR studies using a ^{15}N-guanine-labeled derivative suggested that Rz28 contains tandem G:A pairs that are not of the side-by-side type which is found in the crystal structure of hammerhead ribozyme complexes. Comparison of the HMQC spectra of ^{15}N-guanine-labeled Rz28 and Rz24 suggested that Rz24 also contains the same type of tandem G:A pairs.

Key words: G:A pair, hairpin, NMR, ribozyme, RNA.

The active domain of a hammerhead ribozyme consists of three double-stranded stems (stems I, II, and III), two internal loops (residues 3-9 and 12-14) that contain most of the conserved bases for the ribozyme and a bulge (residue 17) (*1-3*) (Fig. 1a). A ribozyme system can be divided into two components, a substrate and an enzyme. The enzyme catalytically cleaves the substrate RNA at the bulge-stem I junction (shown with an arrow in Fig. 1) in the presence of Mg^{2+} ions through intramolecular transesterification of the 3′-5′ phosphodiester, producing a 2′,3′-cyclic phosphate diester. The mechanism of catalysis for hammerhead ribozymes has been studied by many means, mostly with chemical and biochemical techniques. Structural studies by NMR (*2, 4, 5*) and X-ray crystallography (*6, 7*) have been reported. The NMR studies revealed that hammerhead ribozymes indeed take on the secondary structure expected for the hammerhead motif. The X-ray studies revealed that stems III and II form a continuous helix and stems I and II are positioned side by side and relatively close to each other. At the junction of co-linear stems III and II, side-by-side type tandem G:A base pairs (Fig. 2b) are observed. Some metal ion-binding sites are also found in the crystals. However, the precise molecular mechanism of hammerhead ribozyme action is unknown.

Stem II can be replaced by a loop (*8, 9*) or non-nucleotidic linker (*10, 11*). Since a small system is preferable for elucidation of the solution structure of hammerhead ribozyme by NMR, to simplify the spectrum, we designed a mutant ribozyme (Fig. 1b) in which stem II of the parent ribozyme (*2, 12, 13*) (Fig. 1a) is replaced by a UUUU loop and examined its properties (*14, 15*). It turned out that the mutant ribozyme has a reduced activity because of a lower affinity for Mg^{2+} ions, but shows cleavage activity comparable to that of the parent ribozyme in the presence of 100 mM $MgCl_2$. In the course of these studies, we found that in the transcription reaction by T7 RNA polymerase to synthesize the 24-mer enzyme component (**Rz24**) (Fig. 1c), a longer RNA is obtained as a major product. The longer RNA was identified as a 28-mer (**Rz28**) (Fig. 1d) with 4 extra nucleotides added at the 3′-terminus of **Rz24**, the sequence of which is complementary to that of the 5′-terminal 4 nucleotide sequence of **Rz24**.

In this paper, we report a structural study of **Rz28**, mainly by NMR using a ^{15}N-guanine labeled derivative for signal assignment. **Rz28** appears to take a hairpin structure much more stable than that of **Rz24**. Elucidation of the conformation of **Rz28** may provide a basis for understanding the conformation of **Rz24**. Both RNA oligomers have a

[1] This research was supported in part by Grants-in-Aid for Scientific Research on Priority Areas (#05265211, #05244101, #06276103, #08249212, #08680715) from the Ministry of Education, Science, Sports and Culture of Japan and by the Proposal-Based Advanced Industrial Technology R&D Program from the New Energy and Industrial Technology Development Organization (NEDO) of Japan. M.K. was supported by grants from the Kanagawa Academy of Science Technology and Kato Memorial Bioscience Foundation.

[2] To whom correspondence should be addressed. Fax: +81-45-339-4265, E-mail: uesugi@mac.bio.bsk.ynu.ac.jp

Abbreviations: FID, free induction decay; HMQC, heteronuclear multi-quantum coherence; NOE, nuclear Overhauser effect; NOESY, nuclear Overhauser effect spectroscopy; NTP, ribonucleoside triphosphate; PEG, polyethylene glycol; Rz24, ribozyme 24-mer; Rz28, ribozyme 28-mer; TPPI, time proportional phase incrementation.

sequence which can form a tandem G:A base pair at the junction of a double-helical stem and a loop. The NMR study revealed that **Rz28** forms a stable hairpin structure containing tandem G:A pairs, which are not of the side-by-side type as found in the crystal structure of hammerhead ribozyme complexes, at the junction of the stem and loop. Comparison of the 2D HMQC spectra of ^{15}N-guanine-labeled **Rz28** and **Rz24** suggested that **Rz24** also contains tandem G:A base pairs of the same type.

MATERIALS AND METHODS

Preparation of RNA—Except for Tris-HCl, all solutions were treated with diethyl pyrocarbonate to inactivate trace ribonucleases, and autoclaved. The RNA oligomers, **Rz24** and **Rz28**, were synthesized by *in vitro* transcription with T7 RNA polymerase using fully double-stranded promoter-template DNA. The DNA oligomers were synthesized using a DNA synthesizer (model 392, Applied Biosystems). T7 RNA polymerase was prepared from *Escherichia coli* BL21 cells carrying the plasmid, pAR1219 (*16*). Transcription reaction was carried out at 37°C for 6 h according to the procedure of Milligan *et al.* (*17*) with some modification. The reaction mixture comprised 2 μM DNA promoter-template, 0.1 mg/ml T7 RNA polymerase, 7.5 mM each NTP, 35 mM $MgCl_2$, 40 mM Tris-HCl (pH 8.1), 5 mM DTT, 2 mM spermidine, 0.1% Triton X-100 (v/v), and 80 mg/ml PEG8000. For the preparation of ^{15}N-G-labeled oligomers, uniformly labeled ^{15}N-GTP, which was purchased from Nippon Sanso (Tokyo), was used. After transcription, the crude RNA was subjected to preparative denaturing (7 M urea) 10% polyacrylamide gel electrophoresis. The product oligomers were located by UV shadowing, isolated from the gel by electro-elution, and desalted by using Centricon (exclusion molecular weight 3,000) (Amicon). For sequence analysis, the oligomers were labeled by kination of the 5′-terminal OH with T4 polynucleotide kinase (Takara Shuzo, Kyoto) and [γ-^{32}P]ATP (about 6,000 Ci/mmol). The labeled RNA was subjected to partial alkaline hydrolysis (*18*) and partial digestion with RNase T_1, RNase U_2, RNase *phyM* and *Bacillus cereus* RNase (Pharmacia). The digestion products were separated by denaturing 20% polyacrylamide gel electrophoresis and identified by comparison of the product bands. The yield and concentration of RNAs were calculated from the UV absorbance at 260 nm using the molar absorption coefficients of the component nucleotides.

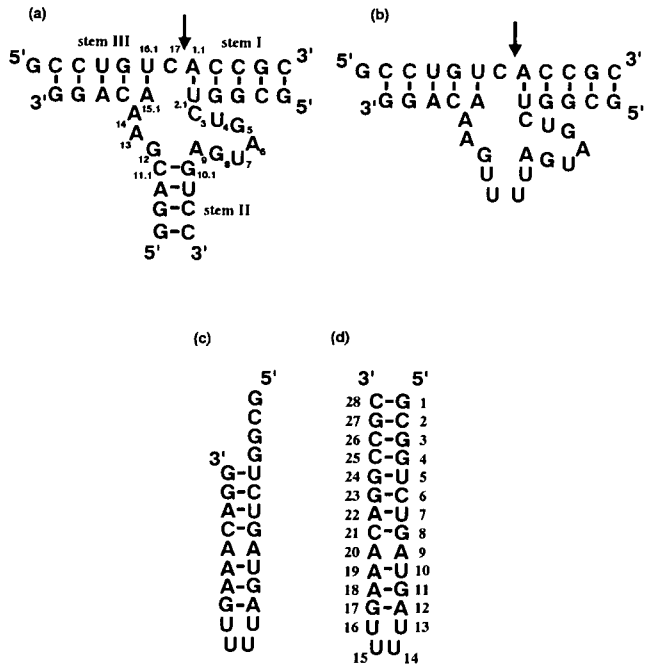

Fig. 1. **Structure of the hammerhead ribozyme complexes and related oligonucleotides.** (a) The parent ribozyme complex, (b) the mutant ribozyme complex with deletion of stem II, (c) the enzyme component (**Rz24**) of the mutant ribozyme complex, (d) the major product oligonucleotide in the transcription with T7 RNA polymerase (**Rz28**).

Limited Digestion of Rz28 with Secondary-Structure-Specific RNases—After dephosphorylation with alkaline phosphatase, **Rz28** was labeled at the 5′-terminus by phosphorylation with T4 polynucleotide kinase and [γ-^{32}P]ATP. The labeled **Rz28** was subjected to limited digestion with double-stranded-RNA-specific RNase V_1 and single-strand-specific mung bean nuclease. For digestion with RNase V_1, **Rz28** was dissolved in 20 mM Tris-HCl buffer (pH 7), 0.2 M NaCl, annealed by heating at 90°C for 3 min and cooling gradually to 37°C, and incubated with the enzyme (0.02 unit/μl) and 10 mM $MgCl_2$ at 37°C for 15 min (*19*). For digestion with mung bean nuclease, **Rz28** was dissolved in 30 mM sodium acetate buffer (pH 7), 50 mM NaCl, annealed in the same manner as described above, and

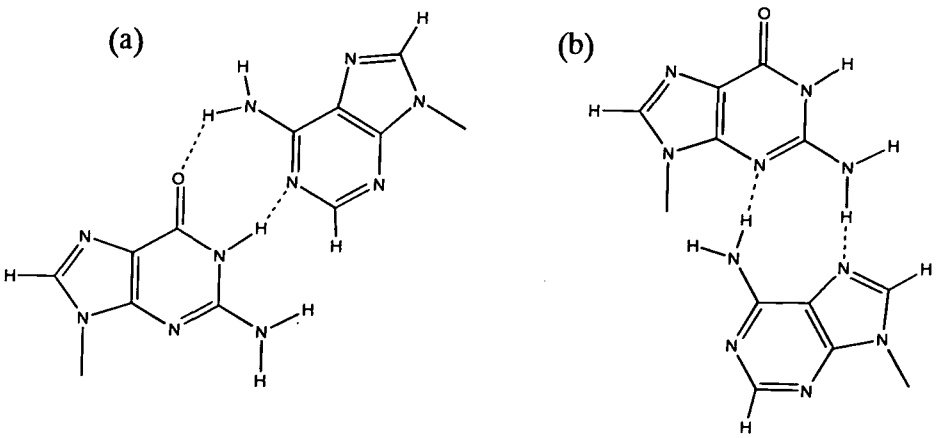

Fig. 2. **Mode of G:A base pairing.** (a) head-to-head type, (b) side-by-side type.

incubated with the enzyme (0.2 unit/μl) and 1 mM $ZnCl_2$ at 37°C for 15 min (*19*).

Measurement of CD-Temperature Profile—CD-temperature profile was recorded on a J-720 spectropolarimeter (JASCO, Tokyo). The **Rz28** samples (1 and 10 μM) were prepared in 10 mM sodium phosphate buffer (pH 7.5), 100 mM NaCl, and annealed by heating at 90°C for 3 min and cooling gradually to 5°C. The temperature was raised from 5 to 80°C at a rate of 50°C/h, and the ellipticity at 265 nm was monitored.

Measurement of NMR Spectra—NMR spectra were recorded on Bruker AM-400 and AMX-500 spectrometers at probe temperatures between 5 and 60°C. **Rz28** (1 mM) was dissolved in 10 mM sodium phosphate buffer (pH 7.5), 100 mM NaCl containing 5% D_2O. The concentration of the ^{15}N-labeled sample was 0.2 mM. The chemical shifts for ^1H and ^{15}N were referenced to the methyl proton resonance of sodium 2,2-dimethyl-2-silapentane-5-sulfonate (internal reference) and to the resonance of $^{15}NH_4Cl$ saturated in water (27.34 ppm) (external reference), respectively. 1D-NOE experiments were carried out with selective irradiation (60 dB below 5W) for 1 s; 400 free induction decays (FIDs) with 16 K data points for 30 ppm were accumulated and a line broadening of 10 Hz was applied. For 2D-NOESY experiments with a mixing time of 150 ms, FIDs (704 scans each) of 2,048 data points in the t_2 domain were collected for 256 data points in the t_1 domain in the phase-sensitive mode, using the States-TPPI method (*20*). By zero-filling the t_1 domain and 90°-shifted sine-bell apodization in both the t_1 and t_2 domains followed by Fourier transformation, spectra of 2,048×512 data points were obtained. For the HMQC experiments, the interpulse delay of 4 ms was used and ^{15}N-decoupling was performed according to the GARP scheme (*21*) with a 90° pulse of 250 μs. For 2D-HMQC experiments, FIDs (64 scans each) of 4,096 data points in the t_2 domain were collected for 512 data points in the t_1 domain in the phase-sensitive mode, using the States-TPPI methods (*20*). By zero-filling the t_1 domain and 90°-shifted sine-bell apodization in both the t_1 and t_2 domains followed by Fourier transformation, spectra of 2,048×1,024 data points were obtained. Spectral width for ^{15}N was 100 ppm. For all experiments, the jump-and-return pulse (*22*) with an interpulse delay of 50 μs was used for suppression of the water resonance.

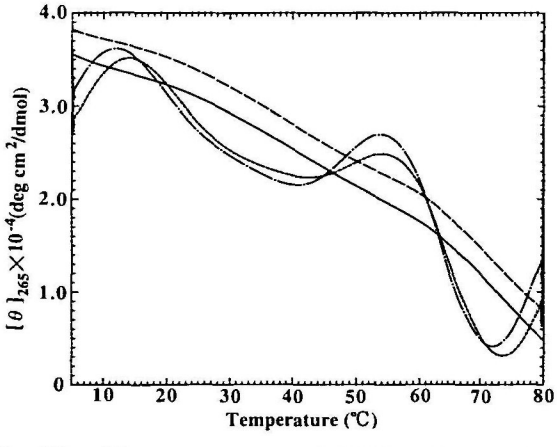

Fig. 3. **CD melting curve measured at 265 nm for Rz28.** Concentration of Rz28 was 1 μM (—; the derivative curve, ·····) or 10 μM (----; the derivative curve, -----) in 10 mM sodium phosphate buffer (pH 7.5), 100 mM NaCl.

RESULTS AND DISCUSSION

Preparation of RNA Oligomers—To synthesize the enzyme component of a mutant hammerhead ribozyme with deletion of stem II (Fig. 1b), transcription with T7 RNA polymerase of an appropriate promoter-template DNA was carried out. Analysis of the RNA products by denaturing polyacrylamide gel electrophoresis showed multiple bands in the region where the product 24-mer (**Rz24**) is expected to be present. Sequence analysis of the oligomers isolated from these bands revealed that a 28-mer RNA (**Rz28**, Fig. 1d) is a major product; a 200-μl reaction yielded 6 nmol of **Rz28** (apparent turnover number, 15; efficiency of GTP incorporation, 5%) and 1 nmol of **Rz24**. These results can be explained by assuming that the primary product, **Rz24**, forms a hairpin with a 5′-overhang (Fig. 1c) and T7 RNA polymerase continues to transcribe using the 5′-overhanging RNA segment as an alternative template. A similar phenomenon, involving RNA template-directed RNA synthesis, was reported by Cazenave and Uhlenbeck (*23*).

Probing the Conformation of Rz28—To confirm that **Rz28** takes a hairpin structure, the effect of the oligomer concentration (1 and 10 μM) on the melting temperature (T_m) was examined by monitoring the CD intensity at 265 nm (Fig. 3). Both solutions showed almost the same T_ms (at around 40 and 70°C) suggesting that the T_m is independent of oligomer concentration and therefore **Rz28** takes a hairpin conformation.

The secondary conformation was further probed by limited digestion experiments with double-strand-region-

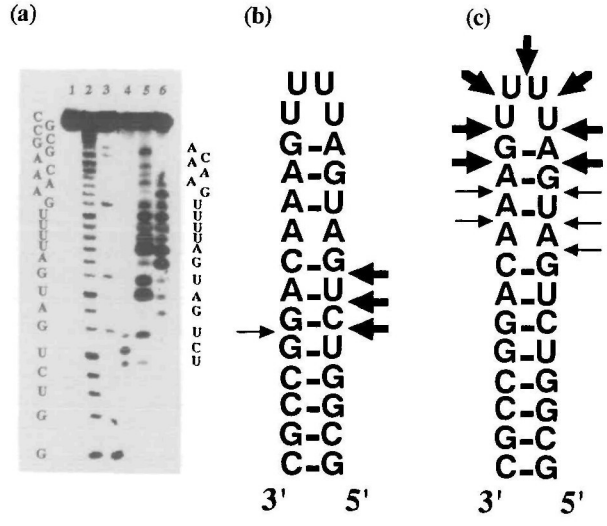

Fig. 4. **Analysis of secondary structure of Rz28 by limited digestion.** (a) **Rz28** (lane 1) was subjected to partial digestion with alkali (lane 2), RNase T_1 in the presence 7 M urea (lane 3), RNase V_1 (lane 4), or mung bean nuclease (lanes 5 and 6). Digestion was carried out shortly after annealing (lane 5) or after leaving the annealed sample at 20°C for 12 h (lane 6). The results were examined by denaturing polyacrylamide gel electrophoresis. (b) Cleavage sites with RNase V_1. (c) Cleavage sites with mung bean nuclease. The thick arrows indicate the strong cleavage sites and the thin arrows indicate the weak cleavage sites.

specific RNase V_1 and single-strand-region-specific mung bean nuclease (Fig. 4). These enzymes cleave RNA producing fragments with newly formed 3′-OH and 5′-phosphate groups. Specific cleavage with RNase V_1 was observed in the middle of the possible stem region (lane 4). On the other hand, cleavage with mung bean nuclease was observed mainly around the possible loop region (lanes 5 and 6). In this case, when digestion was carried out shortly after annealing as usual (lane 5), additional cleavage at A9 and U10 (see Fig. 1d) was noted. These cleavage sites were not observed when the annealed sample was kept at 20°C for 12 h prior to the enzyme addition (lane 6). These results may suggest that A9 residue bulges out shortly after annealing but is incorporated into the double helical stem during prolonged storage. The hairpin conformation of **Rz28** was confirmed by these experiments.

The RNA cleavage activity of **Rz28** was examined under standard conditions [substrate 12-mer (1 μM) and enzyme (1 μM) in 50 mM Tris-HCl buffer (pH 8) at 37°C] (*15*). The substrate was cleaved to the extent of about 10% with 10 mM $MgCl_2$ and about 40% with 100 mM $MgCl_2$ in 20 min while, in the case of **Rz24**, the substrate was cleaved by about 20% with 10 mM $MgCl_2$ and by about 60% with 100 mM $MgCl_2$ in 20 min (*15*). This result shows that the activity of **Rz28** is lower than, but comparable to that of **Rz24**. This is rather surprising because **Rz28** itself shows a T_m at around 70°C even in the absence of $MgCl_2$. The T_m curve for **Rz28** shows that some region in the hairpin, probably the region around the G:A pairs, melts at around 40°C. In the reaction mixture at 37°C, the partially melted region of **Rz28** may initiate formation of an active complex with the substrate which rapidly produces the cleaved products.

NMR Spectra of ^{15}N-Guanine-Labeled Rz28—NMR spectra in the imino proton region of **Rz28**, in which all the guanosine residues are ^{15}N-labeled, are shown in Fig. 5. The spectrum without ^{15}N-decoupling (Fig. 5a) contains doublet imino proton signals due to ^{15}N-^{1}H coupling of ^{15}N-labeled guanosine residues. The spectrum with ^{15}N-decoupling (Fig. 5b) corresponds to the spectrum of the non-labeled **Rz28**. The 1D-HMQC spectrum (Fig. 5c) contains only the imino proton (^{15}N-H) signals of the labeled guanosine residues: signals b–h, j, and k. The imino proton signals of uridine residues can be identified by comparison of Fig. 5b with Fig. 5c: signals a, b, i, l, and m; signal b contains two resonances, one from a guanosine residue and the other from a uridine residue.

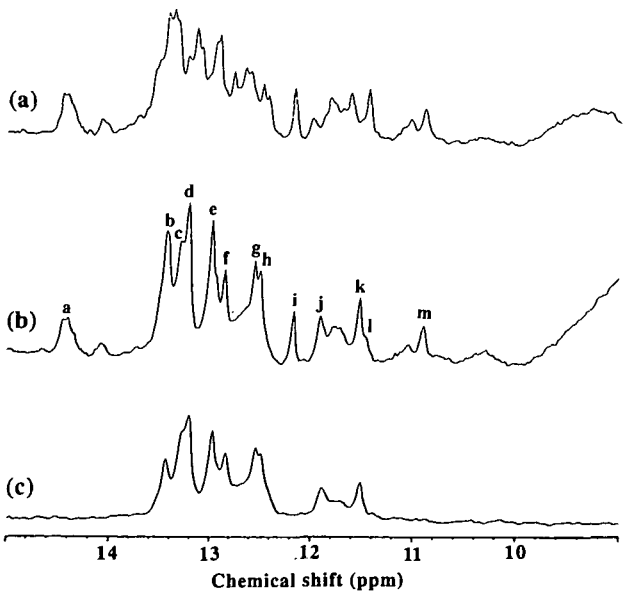

Fig. 5. **NMR spectra of Rz28 (0.2 mM), in which all the guanosine residues are ^{15}N-labeled, in the imino proton region.** (a) Spectrum without ^{15}N-decoupling. (b) Spectrum with ^{15}N-decoupling. (c) 1D-HMQC spectrum. Measured in 10 mM sodium phosphate buffer (pH 7.5), 100 mM NaCl containing 5% D_2O at 5°C.

Assignment of the Imino Proton Signals—The imino proton signals were further assigned by analysis of 2D-NOESY and 1D-NOE data. The 2D-NOESY spectrum in the imino proton-imino proton region is shown in Fig. 6. A

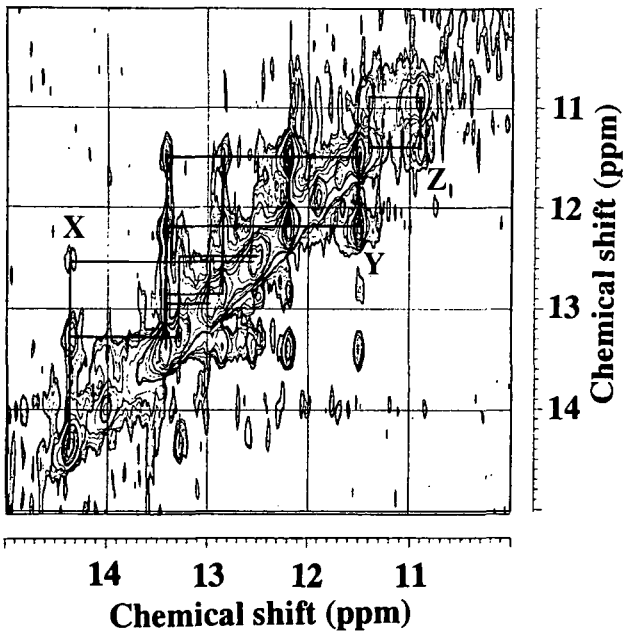

Fig. 6. **2D-NOESY spectrum of Rz28 (1 mM) in the imino proton-imino proton region.** Measured in 10 mM sodium phosphate buffer (pH 7.5), 100 mM NaCl containing 5% D_2O at 10°C. The straight lines indicate tracing of the NOEs for sequential assignment and an NOE between signals l and m. NOEs labeled X, Y, and Z are those between signals a and g, i and k, and l and m, respectively.

TABLE I. **Summary of the imino proton signal assignments for Rz28.**

Signal	Chemical shift (ppm)	Assignment	Observed NOE[a]
a	14.20	U10	c and g
b	13.44	G4 and U7	e, f, g*, i, and k
c	13.29	G11	a and h
d	13.22	G27	e*
e	12.99	G3	b
f	12.86	G23	b, i, and k
g	12.56	G8	a and b*
h	12.50	G17	c
i	12.18	U5	b, f, and k
j	11.91	G1	
k	11.49	G24	b, f, and i
l	11.42	U	m
m	10.89	U	l

[a]NOE connectivities observed in the 1D-NOE difference spectra are indicated by asterisks.

strong NOE peak (signal Y) is observed between signals i (from NH of U) and k (from NH of G). This result and the chemical shifts of signals i (12.18 ppm) and k (11.49 ppm) suggest that these signals are due to a G:U base pair; signals i and k can be assigned to the imino protons of U5 and G24, respectively. Starting from these signals, other signals can be sequentially assigned; i- or k-b-e-d in the 5′-direction and i- or k-f-b-g-a-c-h in the 3′-direction (Fig. 7 and Table I). The NOEs between signals d and e, and between signals b and g, which were not clearly seen in the 2D-NOESY spectrum, were confirmed by 1D-NOE data (Fig. 8). When signal d was irradiated, a significantly larger peak was observed on signal e with respect to that on signal b, which is due to leakage of the irradiation power, whereas the resonance frequence difference between signals d and e is rather larger than that between signals d and b (Fig. 8a). Irradiation of signal b gave an NOE peak on signal f as well as on the other expected signals (Fig. 8b). The remaining signal j did not show any significant NOE. This signal was tentatively assigned as that of G1, the 5′-terminal residue, since it disappeared earlier (at around 30°C) than the other signals upon raising the temperature (data not shown).

Conformation of Rz28 Hairpin—A weak NOE (signal X in Fig. 6) was observed between the imino protons of G8 and U10. This result suggests that the bases of G8 and U10 are stacked and the A9 base is flipped out from the double-helical stem, and is consistent with the result of the limited digestion experiment (Fig. 4, lane 5) with mung bean nuclease, where the digestion was carried out shortly after annealing. It should also be noted that a clear NOE (signal Z in Fig. 6) is observed between signals l and m; both signals are due to uridine residues (see Fig. 5). We assume that these signals are from imino protons of uridines of the UUUU loop (probably U13 and U16) and that the uracil bases form a U:U base pair; the possible presence of a U:U pair has been reported for an internal loop of a 27-nucleotide duplex with 5S rRNA sequences (*24*).

The imino protons of G11:A18 and G17:A12 pairs show chemical shifts of 13.29 ppm and 12.50 ppm, respectively. These chemical shift values strongly suggest that the geometry of these tandem G:A pairs is not of the side-by-side type (Fig. 2b). Although we were not able to observe an NOE between N1H of G and C2H of A under the conditions examined, it is highly probable that the tandem G:A pairs are of head-to-head type (Fig. 2a), as discussed below. It is difficult to observe this NOE for a head-to-head G:A pair if the G:A pair is not greatly stabilized (*31-33*). Tandem G:A pairs in oligonucleotide duplexes are reported to show the guanine imino proton signals either at 10-10.5 ppm (*25-30*) or at around 12.5 ppm (*26, 29, 31*). The signals at higher field (10-10.5 ppm) are assigned to guanine imino protons, which are not hydrogen-bonded, of side-by-side G:A base pairs. In this case, the duplexes contain common sequences, YGAR:YGAR. The only exception is a duplex containing YGAY:RGAR (*27*). The signals at lower field (around 12.5 ppm) are assigned to guanine imino protons, which are hydrogen-bonded, of head-to-head G:A base pairs. In this case, the duplexes contain RGAY:RGAY sequences. In the present case, **Rz28** contains YGAY and YGAR sequences at the junction of a double-stranded stem and a loop. The presence of a YGAY sequence and the location at a stem-loop junction may not be favorable for formation of side-by-side, tandem G:A pairs, which are most stabilized by the sequences, YGAR:YGAR, in a duplex (*27*). Molecular model building analysis shows that

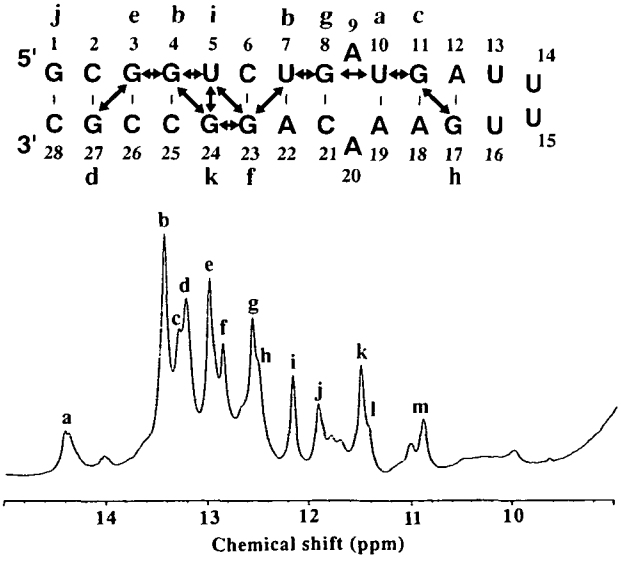

Fig. 7. **Assignments of the imino proton signals and observed NOEs.** The observed NOEs are indicated with double-headed arrows.

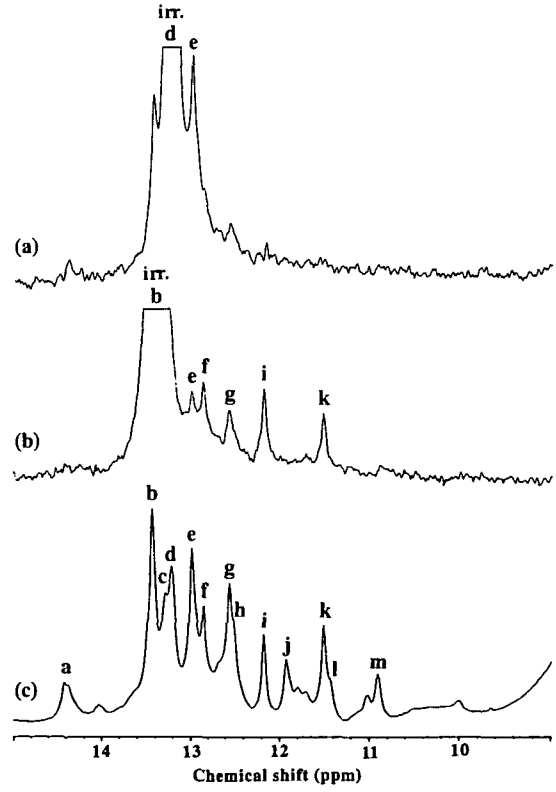

Fig. 8. **1D-NOE difference spectra for Rz28 (1 mM).** Measured in 10 mM sodium phosphate buffer (pH 7.5), 100 mM NaCl containing 5% D_2O at 10°C. (a) and (b), NOE difference spectra; (c) normal spectrum. The irradiated signals are indicated at the top of the spectra. Observed NOEs are indicated by the name of the signals (Fig. 6).

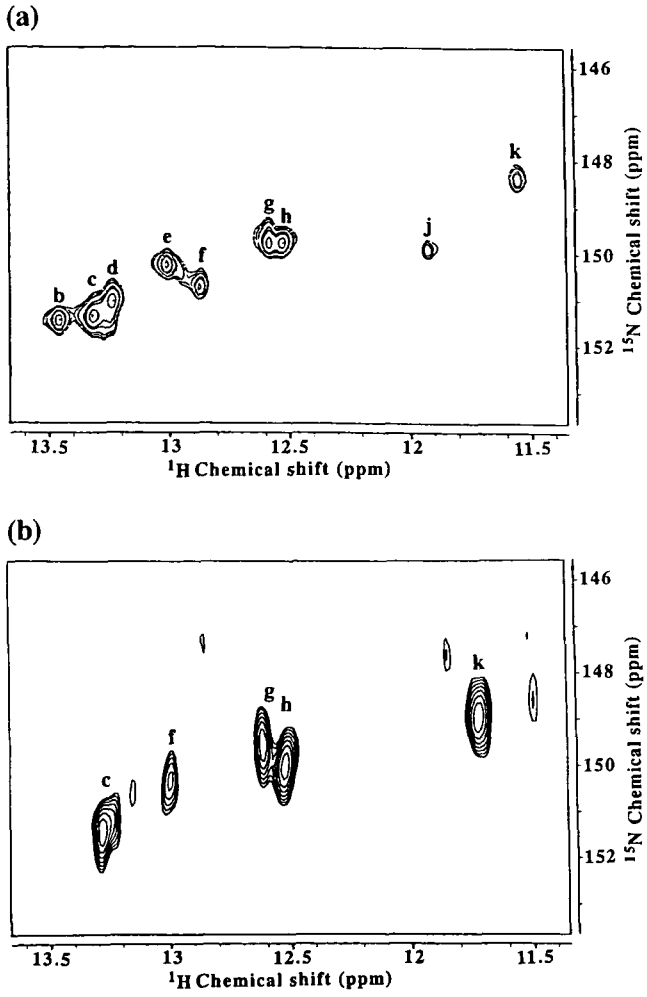

Fig. 9. **2D-HMQC spectra of Rz28 (0.2 mM) (a) and Rz24 (0.04 mM) (b), in which all the guanosine residues are ^{15}N-labeled, in the imino proton-imino nitrogen region.** Measured in 10 mM sodium phosphate (pH 7.5), 100 mM NaCl containing 5% D_2O at 5°C.

the Y1G2A3R4:Y4′G3′A2′R1′ segment is stabilized by two columns of vertical stacking interactions, Y1/G2/G3′/Y4′ and R1′/A2′/A3/R4 in the duplex.

Comparison of NMR Spectra of ^{15}N-Guanine-Labeled Rz28 and Rz24—2D HMQC spectra of ^{15}N-G labeled **Rz28** and **Rz24** are shown in Fig. 9. In these spectra, a correlation signal is observed at the cross point of the chemical shifts for an imino proton (^{1}H) and an imino nitrogen (^{15}N) that are directly bonded. Deletion of the 3′-terminal segment, C25 to C28, of **Rz28** results in a loss of the G27 residue as well as hydrogen-bonds of the G1, G3, and G4 residues for **Rz24**; these changes should eliminate the cross peaks corresponding to the hydrogen-bonded imino proton signals d, j, e, and b, respectively, which are observed for **Rz28**. Comparison of the 2D HMQC spectra of **Rz28** and **Rz24** (Fig. 9, a and b, respectively) suggests that the spectrum of **Rz24** can be explained by these changes. The proton chemical shifts for signals k and f (Fig. 9), which are due to the 3′-terminal and penultimate residues of **Rz24**, G24 and G23, seem to be affected considerably by the loss of the 3′-terminal segment of **Rz28**. These results for **Rz24** in turn confirm the signal assignments for **Rz28**.

CONCLUSIONS

The secondary structure of an RNA oligonucleotide (**Rz28**), which contains a sequence of the enzyme component of a mutant hammerhead ribozyme system, has been examined by enzymatic and NMR methods. The results reveal that **Rz28** forms a hairpin structure which contains tandem G:A pairs at the junction of a stem and a loop. The G:A pairs are assumed to take on a head-to-head type arrangement (Fig. 2a) rather than a side-by-side type arrangement (Fig. 2b). **Rz24**, which is the enzyme component without an extra sequence in the 3′-terminus, is also assumed to take on the same base-pair conformation. The presence of such tandem G:A pairs is not known for hammerhead ribozyme systems. Side-by-side type tandem G:A pairs are found in the crystal structure of hammerhead ribozyme systems (*6, 7*). The presence of G:A pairs of this type was also reported for the enzyme components of hammerhead ribozyme systems in the absence of Mg^{2+}, based on an NMR study (*34, 35*). It should be noted that, in these NMR studies, stem II is closed with a "tetranucleotide loop" which can form a very stable hairpin.

However, the side-by-side tandem G:A pairs, in which the 2-amino groups of guanine residues and 6-amino and N7 groups of adenine residues are involved in hydrogen-bonding, seem not to be necessary for catalytic activity of hammerhead ribozymes (*36-40*). Replacement of A9 with purine riboside or 7-deaza-A (*36-39*), and of G8 with inosine (*37-40*) does not profoundly reduce the substrate RNA cleavage rate. On the other hand, it is known that replacement of a guanosine with an inosine in DNA duplexes containing side-by-side tandem G:A pairs markedly reduces the stability of the duplex (*25*). Therefore, it is very likely that G:A pairs, which are not of the side-by-side type, play a role in the catalytic activity of hammerhead ribozymes. Further study on the effects of interaction with the substrate component and Mg^{2+} ions in the present system is needed to clarify this point.

We wish to thank Professor H. Akutsu for giving us the opportunity to use his NMR machine. We also thank Dr. M. Orita, Mr. T. Ohtsuki, and Mr. M. Nagaoka for helpful advice.

REFERENCES

1. Uhlenbeck, O.C. (1987) A small catalytic oligoribonucleotide. *Nature* **328**, 596-600
2. Odai, O., Kodama, H., Hiroaki, H., Sakata, T., Tanaka, T., and Uesugi, S. (1990) Synthesis and NMR study of ribooligonucleotides forming a hammerhead-type RNA enzyme system. *Nucleic Acids Res.* **18**, 5955-5960
3. Hertel, K.J., Pardi, A., Uhlenbeck, O.C., Koizumi, M., Ohtsuka, E., Uesugi, S., Cedergren, R., Eckstein, F., Gerlach, W.L., Hodgson, R., and Symons, R.H. (1992) Numbering system for the hammerhead. *Nucleic Acids Res.* **20**, 3252
4. Heus, H.A. and Pardi, A. (1991) Nuclear magnetic resonance studies of the hammerhead ribozyme domain: Secondary structure formation and magnesium ion dependence. *J. Mol. Biol.* **217**, 113-124
5. Pease, A.C. and Wemmer, D.E. (1990) Characterization of the secondary structure and melting of a self-cleaved RNA hammerhead domain by ^{1}H NMR spectroscopy. *Biochemistry* **29**, 9039-9046
6. Pley, H.W., Flaherty, K.M., and McKay, D.B. (1994) Three-dimensional structure of a hammerhead ribozyme. *Nature* **372**,

68-74
7. Scott, W.G., Finch, J.T., and Klug, A. (1995) The crystal structure of an all-RNA hammerhead ribozyme: A proposed mechanism for RNA catalytic cleavage. *Cell* **81**, 991-1002
8. McCall, M.J., Hendry, P., and Jennings, P.A. (1992) Minimal sequence requirements for ribozyme activity. *Proc. Natl. Acad. Sci. USA* **89**, 5710-5714
9. Tuschl, T. and Eckstein, F. (1993) Hammerhead ribozymes: Importance of stem-loop II for activity. *Proc. Natl. Acad. Sci. USA* **90**, 6991-6994
10. Thomson, J.B., Tuschl, T., and Eckstein, F. (1993) Activity of hammerhead ribozymes containing non-nucleotidic linkers. *Nucleic Acids Res.* **21**, 5600-5603
11. Benseler, F., Fu, D.J., Ludwig, J., and McLaughlin, L.W. (1993) Hammerhead-like molecules containing non-nucleoside linkers are active RNA catalysts. *J. Am. Chem. Soc.* **115**, 8483-8484
12. Uesugi, S., Odai, O., Kodama, H., Hiroaki, H., Sakata, T., and Tanaka, T. (1992) Hammerhead-type RNA enzyme and its derivatives which consist of three RNA oligomer strands in *Structure and Function* (Sarma, R.H. and Sarma, M.H., eds.) Vol. 2, pp. 143-158, Adenine Press, Schenectady
13. Odai, O., Hiroaki, H., Sakata, T., Tanaka, T., and Uesugi, S. (1990) The role of a conserved guanosine residue in the hammerhead-type RNA enzyme. *FEBS Lett.* **267**, 150-152
14. Sakamoto, T., Kim, M.H., Kurihara, Y., Sasaki, N., Noguchi, T., Katahira, M., and Uesugi, S. (1997) Characterization of a hammerhead ribozyme with deletion of stem II. *Nucleic Acids Symposium Series* No. 31, 189-190
15. Sakamoto, T., Kim, M.H., Kurihara, Y., Sasaki, N., Noguchi, T., Katahira, M., and Uesugi, S. (1997) Properties of a hammerhead ribozyme with deletion of stem II. *J. Biochem.* **121**, 288-294
16. Davanloo, P., Rosenburg, A.H., Dunn, J.J., and Studier, F.W. (1984) Cloning and expression of the gene for bacteriophage T7 RNA polymerase. *Proc. Natl. Acad. Sci. USA* **81**, 2035-2039
17. Milligan, J.F., Groebe, D.R., Witherell, G.W., and Uhlenbeck, O.C. (1987) Oligoribonucleotide synthesis using T7 RNA polymerase and synthetic DNA template. *Nucleic Acids Res.* **15**, 8783-8798
18. Kuchino, Y. and Nishimura, S. (1989) Enzymatic RNA sequencing in *Methods in Enzymology* (Dahlberg, J.E. and Abelson, J.N., eds.) Vol. 180, pp. 154-163, Academic Press, New York
19. Knapp, G. (1989) Enzymatic approaches to probing of RNA secondary and tertiary structure in *Methods in Enzymology* (Dahlberg, J.E. and Abelson, J.N., eds.) Vol. 180, pp. 192-212, Academic Press, New York
20. Marion, D., Ikura, M., Tschudin, R., and Bax, A. (1989) Rapid recording of 2D NMR spectra without phase cycling. Application to the study of hydrogen exchange in protein. *J. Magn. Reson.* **85**, 393-399
21. Shaka, A.J., Barker, P.B., and Freeman, R. (1985) Computer optimized decoupling scheme for wideband applications and low-level operation. *J. Magn. Reson.* **64**, 547-552
22. Plateau, P. and Gueron, M. (1982) Exchangeable proton NMR without base-line distortion, using new strong-pulse sequences. *J. Am. Chem. Soc.* **104**, 7310-7311
23. Cazenave, C. and Uhlenbeck, O.C. (1994) RNA template-directed RNA synthesis by T7 RNA polymerase. *Proc. Natl. Acad. Sci. USA* **91**, 6972-6976
24. Wimberly, B., Varani, G., and Tinoco, I., Jr. (1993) The conformation of loop E of eukaryotic 5S ribosomal RNA. *Biochemistry* **32**, 1078-1087
25. Li, Y., Zon, G., and Wilson, W.D. (1991) NMR and molecular modeling evidence for a G:A mismatch base pair in a purine-rich DNA duplex. *Proc. Natl. Acad. Sci. USA* **88**, 26-30
26. Cheng, J.W., Chou, S.H., and Reid, B.R. (1992) Base pairing geometry in GA mismatches depends entirely on the neighboring sequence. *J. Mol. Biol.* **228**, 1037-1041
27. Katahira, M., Sato, H., Mishima, K., Uesugi, S., and Fujii, S. (1993) NMR studies of G:A mismatches in oligodeoxyribonucleotide duplexes modelled after ribozymes. *Nucleic Acids Res.* **21**, 5418-5424
28. Katahira, M., Kanagawa, M., Sato, H., Uesugi, S., Fujii, S., Kohno, T., and Maeda, T. (1994) Formation of sheared G:A base pairs in an RNA duplex modeled after ribozymes, as revealed by NMR. *Nucleic Acids Res.* **22**, 2752-2759
29. Greene, K.L., Jones, R.L., Li, Y., Robinson, H., Wang, A.H.J., Zon, G., and Wilson, W.D. (1994) Solution structure of a G:A mismatch DNA sequence, $d(CCATGAATGG)_2$, determined by 2D NMR and structural refinement methods. *Biochemistry* **33**, 1053-1062
30. SantaLucia, J., Jr. and Turner, D. (1993) Structure of $(rGGCGAGCC)_2$ in solution from NMR and restrained molecular dynamics. *Biochemistry* **32**, 12612-12623
31. Kan, L.S., Chandrasegaran, S., Pulford, S.M., and Miller, P.S. (1983) Detection of a guanine:adenine base pair in a decadeoxyribonucleotide by proton magnetic resonance spectroscopy. *Proc. Natl. Acad. Sci. USA* **80**, 4263-4265
32. Katahira, M., Kanagawa, M., and Uesugi, S. (1994) Drastic difference in G:A base pairing between two consecutive G:A mismatches and a single G:A mismatch in DNA. *Nucleosides Nucleotides* **13**, 1507-1515
33. Carbonnaux, C., van der Marel, G.A., van Boom, J.H., Guschlbauer, W., and Fazakerley, G.V. (1991) Solution structure of an oncogenic DNA duplex containing a G·A mismatch. *Biochemistry* **30**, 5449-5458
34. Orita, M., Vinayak, R., Andrus, A., Warashina, M., Chiba, A., Kaniwa, H., Nishikawa, F., Nishikawa, S., and Taira, K. (1996) Magnesium-mediated conversion of an inactive form of a hammerhead ribozyme to an active complex with its substrate. *J. Biol. Chem.* **271**, 9447-9454
35. Simorre, J.-P., Legault, P., Hangar, A.B., Michiels, P., and Pardi, A. (1997) A conformational change in the catalytic core of the hammerhead ribozyme upon cleavage of an RNA substrate. *Biochemistry* **36**, 518-525
36. Fu, D.-J. and McLaughlin, L.W. (1992) Importance of specific adenosine N^7-nitrogens for efficient cleavage by a hammerhead ribozyme. A model for magnesium binding. *Biochemistry* **31**, 10941-10949
37. Fu, D.-J. and McLaughlin, L.W. (1992) Importance of specific purine amino and hydroxyl groups for efficient cleavage by a hammerhead ribozyme. *Proc. Natl. Acad. Sci. USA* **89**, 3985-3989
38. Fu, D.-J., Rajur, S.B., and McLaughlin, L.W. (1993) Importance of specific guanosine N^7-nitrogens and purine amino groups for efficient cleavage by a hammerhead ribozyme. *Biochemistry* **32**, 10629-10637
39. Slim, G. and Gait, M.J. (1992) The role of the exocyclic amino groups of conserved purines in hammerhead ribozyme cleavage. *Biochem. Biophys. Res. Commun.* **183**, 605-609
40. Tuschl, T., Ng, M.M.P., Pieken, W., Benseler, F., and Eckstein, F. (1993) Importance of exocyclic base functional groups of central core guanosines for hammerhead ribozyme activity. *Biochemistry* **32**, 11658-11668